PCCP

Rotational spectroscopy of 2,4,6-cycloheptatriene-1-carbonitrile: Facilitating the search for complex cyclic molecules in the ISM[†]

Gayatri Batra,[a,b] Laura Pille,[a] Benjamin E. Arenas,[a‡] and Melanie Schnell[a,b*]

The recent astronomical observations of the simplest aromatic nitrile benzonitrile, c-C_6H_5CN, followed by a five-membered and a bicyclic CN-functionalized ring in TMC-1 have provided a significant impetus to the field for searches of cyclic complex organic molecules in space. One such example is 2,4,6-cycloheptatriene-1-carbonitrile, a seven-membered ring with a -CN group attached to the sp^3-hybridized carbon atom. With a permanent electric dipole moment of 4.3 D, this molecule is an excellent candidate for laboratory rotational spectroscopy. In this study, experiments were performed in the 2-8 GHz, 18-26 GHz and 75-110 GHz frequency ranges in a supersonic expansion setup and a room temperature flow cell setup. The measurements across the broad frequency range of 2-110 GHz have enabled the identification and assignment of the vibronic ground state, singly substituted rare-atom isotopologues, and vibrationally excited states. Here, we report the precise determination of the rotational constants, quartic centrifugal distortion constants, nitrogen nuclear quadrupole coupling constants, as well as molecular structure in its vibronic ground state. The comprehensive rotational spectroscopy study of this molecule, covering a large frequency range, forms the basis for its future astronomical detection and thus for extending the pool of detected complex cyclic molecules.

1 Introduction

The advent of radio astronomy in the late 1960s has facilitated the astronomical detections of well-known as well as highly unusual molecular systems primarily via their rotational signatures, indicating the astonishingly rich chemical inventory present in the interstellar medium (ISM). With the state-of-the-art facilities and high-sensitivity telescopes available today, more complex molecules are becoming the target of astronomical searches[1]. Recent discoveries of new molecular species are not only the subject of chemical curiosity but also underline important open questions. For example, what degree of chemical complexity exists in molecular clouds, what pathways are responsible for their formation, and if there is a correlation between the highly abundant unsaturated linear chains such as polyynes and cyanopolyynes and the comparatively scarcely observed cyclic analogs.[2]

Among the vast array of molecular species, surpassing 300, iden-

tified in the interstellar medium or circumstellar shells [*†], the majority of these detections were made via their rotational spectra. For direct detection via its rotational signature, a molecule must possess a permanent electric dipole moment. As a result, polar molecules, despite their potentially low abundances, serve as sensitive tracers of the molecular gases present in the ISM. This prerequisite of polarity explains the existing predominance in the detection of CN-containing molecules ($> 15\%$ of the total detected molecules so far)[†], as they possess high values of electric dipole moments leading to intense rotational spectra which facilitate their astronomical search.

The terrestrial organic chemistry on Earth is dominated by the presence of molecules containing five- and six-membered rings as building blocks of many biological compounds[3]. However, it was only in the year 2018 that the first cyclic aromatic molecule, the CN-functionalized benzene ring, benzonitrile[4], was identified in the cold starless core TMC-1. This molecule was then subsequently detected in four other prestellar, and possibly protostellar, sources: Serpens 1A, Serpens 1B, Serpens 2, and MC27/L1521F[5], suggesting a high degree of chemical complexity in the early star formation regions. Shortly thereafter, evidence was found for

[a] Deutsches Elektronen-Synchrotron DESY, Notkestr. 85, 22607, Hamburg, Germany.
[b] Institute of Physical Chemistry, Max-Eyth-Str. 1, Christian-Albrechts-Universität zu Kiel, 24118, Kiel, Germany.
[‡] Present address: EaStCHEM School of Chemistry, University of Edinburgh, Dawid Brewster Road, EH9 3FJ, Edinburgh, United Kingdom.
[*] Corresponding author, Email: melanie.schnell.desy.de.

[*] http://www.astrochymist.org/
[†] https://cdms.astro.uni-koeln.de/classic/molecules

cyano-functionalized cyclopentadiene[6] in TMC-1. The detection of the CN-functionalized hydrocarbons can act as a proxy for the unsubstituted molecules as most of the studied reactions of unsaturated hydrocarbons, like benzene, with a CN radical are found to be barrierless and exothermic in nature[7]. The detection of the five-membered and six-membered rings with CN functionalization has evoked interest in investigating the seven-membered CN functionalized ring: 2,4,6-cycloheptatriene-1-carbonitrile (hereafter, CHT-1-CN). In this work, we conducted a thorough rotational spectroscopy study of CHT-1-CN at two different rotational temperatures to facilitate its detection in the cold as well as in warmer regions of the ISM.

In warm regions of the ISM, a considerable proportion of complex molecules reside in low-lying vibrationally excited states. The transitions arising from these vibrationally excited states are commonly referred to as weeds in radio astronomy data[8]. These weeds can occupy many channels in a warm and dense astronomical dataset, and therefore their characterization is an important step in simplifying complex and confusion-limited spectra. Vibrationally excited states, together with isotopologues, constitute a large fraction of the many unidentified lines in the observational datasets, for example, the percentage of these unidentified lines can be as high as 70% in deep observations at Atacama Large Millimeter/submillimeter Array (ALMA) bands 3 and 6, covering 84-116 GHz and 211-275 GHz, respectively[9]. The assignment of vibrationally excited states and isotopologues is also important for the completeness of the astronomical catalogs, especially in the millimeter-wave region. Moreover, isotopologues are important species not only from a spectroscopic but also from a structural point of view. The assignment of singly substituted isotopologues in the rotational spectrum provides the experimentally determined rotational constants, which then lead to the construction of a comprehensive structure of the molecule in the gas phase. For CHT-1-CN, elucidating structural information is of relevance as it is a seven-membered ring with six sp^2- and one sp^3-hybridized carbon atoms. The structures of cycloheptatrienes and their derivatives, investigated with vibrational and rotational spectroscopic techniques, have been a subject of discussion since the early 1960s[10-13].

In this manuscript, we present an extensive analysis of the rotational spectra of CHT-1-CN covering the 2-110 GHz frequency region (in parts of 2-8, 18-26, and 75-110 GHz) in two different experimental settings using the isolated, cold conditions of a supersonic expansion in the 2-26 GHz frequency range and a flow-cell experiment at elevated temperatures (∼323 K) in the 75-110 GHz frequency range. The broad frequency ranges probed and the different experimental conditions employed are of significant importance here, as not only do we analyze the vibronic ground state of the molecule but we also study vibrationally excited states. In addition, the determination of the rotational constants, quartic centrifugal distortion constants, and nuclear quadrupole coupling constants have allowed us to accurately predict the rotational transition frequencies for the ground state into the millimeter-wave region for facilitating astronomical searches.
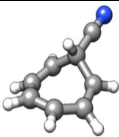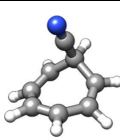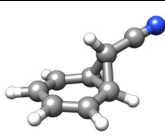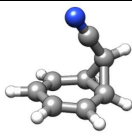
2 Experimental details

The rotational spectra of CHT-1-CN were recorded over a wide frequency range spanning from 2-110 GHz. The comprehensive analysis was achieved using three chirped-pulse Fourier transform rotational spectrometers: the COMPACT spectrometer, operating within 2-18 GHz[14-16], the K-band spectrometer operating within 18-26 GHz[16], and the Brightspec W-band spectrometer operating within 75-110 GHz[17]. The detailed description of the instruments employed here can be found in the given references.

The liquid sample of CHT-1-CN purchased from Sigma Aldrich (with a given chemical purity of $> 95\%$) was used without any further purification. The molecule was first measured in the range of 18-26 GHz using the K-band spectrometer, as for a molecule of this size, most intense transitions simulated with a rotational temperature of 1-3 K lie in the range of the K-band spectrometer. The measurement was extended to the low-frequency range (2-8 GHz) employing the COMPACT spectrometer to better resolve the nuclear hyperfine split transitions due to the presence of the ^{14}N nucleus. For these measurements, the sample of CHT-1-CN was loaded into a modified pulsed nozzle (a modified Parker Series 9 valve equipped with an internal heatable reservoir with an orifice diameter of 1 mm) and heated to ∼311 K. With neon used as a carrier gas at 2.5 bar, the molecular vapor was supersonically expanded into the vacuum chamber. The supersonic expansion of the gas mixture into the vacuum chamber results in a rapid decrease of the rotational temperature, T$_{rot}$, to the range of 1-3 K. In contrast to the spectra recorded in the low-frequency region, the measurement in the high-frequency region (75-110 GHz) was performed under flow-cell conditions. The liquid sample was heated to 323 K resulting in a constant vapor pressure of 2-3 mTorr ($2.6 - 4 \times 10^{-3}$ mbar) in the spectrometer chamber.

A brief description of the measurements performed in this work is given as follows: The COMPACT spectrometer[14-16] was used to record the spectrum in the 2-8 GHz range. A series of eight chirped pulses covering 2-8 GHz (each of 4 μs duration) is generated by the arbitrary waveform generator (AWG) and amplified with a 300 W traveling wave tube amplifier. These excitation pulses are then transmitted into the vacuum chamber containing a package of the supersonically expanded, cold molecules, and the interaction between the molecules and the microwave pulses induces a macroscopic polarization of the molecular ensemble. Eight chirped pulses per gas pulse combined with the gas-pulse repetition rate of 8 Hz led to an effective repetition rate of 64 Hz. Following each excitation, the resulting free induction decays (FIDs) of the macroscopic polarization were recorded for 40 μs. In total, one million FIDs were co-added in the time domain, followed by the fast Fourier transformation into the frequency domain.

The K-band spectrometer, operating in the range of 18-26 GHz[16], uses the combination of the segmented approach and the multi-train method. The bandwidth of 8 GHz is split into smaller segments of 800 MHz, and the spectrum across the whole bandwidth is obtained by stitching these segments together[18]. The multi-train method utilizes multiple pulse trains per molecular gas pulse, increasing the effective repetition rate of the experi-

Table 1 Rotational parameters, electric dipole moment, and relative energies for the calculated lowest energy conformers and tautomers of CHT-1-CN at the B3LYP-D3/aug-cc-pVTZ level of theory.

Rotational parameters	Conformer 1	Conformer 2	Tautomer 1	Tautomer 2
A^a/MHz	3581.7	2277.2	4304.9	2430.1
B/MHz	1252.7	1682.6	1161.1	1733.8
C/MHz	991.1	1538.8	996.7	1627.1
$\mu_a/\mu_b/\mu_c/^b D$	4.3/0.0/0.2	2.8/0.0/2.9	4.3/0.0/0.2	2.5/3.4/0.0
$\Delta E/^c kJ \cdot mol^{-1}$	0.0	6.3	22	24.6

[a] $A, B,$ and C are the rotational constants.
[b] $\mu_a/\mu_b/\mu_c/$ are the electric dipole moment components.
[c] Zero-point energy corrected relative energies.

ment. The AWG synthesizes 1.5 μs long excitation pulses in the range of 7-3 GHz. These chirps are then frequency upconverted to 9-13 GHz and doubled to 18-26 GHz. For each gas pulse, the molecular ensemble is polarized by a series of three pulse trains. The multi-train setup combined with a gas-pulse repetition rate of 10 Hz results in an effective repetition rate of 30 Hz. A total of 2.2 million FIDs were collected (each for a duration of 10 μs), frequency down-converted, co-added, and converted into the frequency domain by fast Fourier transformation.

The W-band spectrometer (75-110 GHz)[17] also utilizes the segmented approach. The 35 GHz bandwidth is covered in segments of 720 MHz each. Among the different measurement modes available, the high dynamic range (HDR) mode was used for this experiment, which addresses each segment of 720 MHz by 30 chirps of 24 MHz bandwidth, thus reducing the spurious content in the collected spectrum. The AWG synthesizes 500 ns excitation pulses in the 1.5-2.3 GHz range, which is then frequency upconverted and multiplied through a series of mixing stages and an active multiplier chain ($\times$6) to produce the radiation in the millimeter-wave regime. A total of one million FIDs (each recorded for 4 μs) were collected followed by conversion into the frequency domain by fast Fourier transformation.

3 Theoretical details and spectroscopic analysis

To explore the conformational flexibility of CHT-1-CN, an automated semi-empirical conformational search was performed with the SPARTAN 14[‡] program using the Austin Model 1 (AM1) method, the Parameterization Method 3 (PM3), and the Parameterization Method 6 (PM6) (Spartan 14). The results from the SPARTAN program combined with chemical intuition yielded two structures differing in the orientation of the cyano group (attached to an sp^3-hybridized carbon atom) with respect to the seven-membered ring. Moreover, the cycloheptatriene ring systems are known to undergo an equilibrium reaction between the norcaradiene–cycloheptatriene forms in the presence of electron-withdrawing groups, such as the cyano group[19].

‡ https://www.wavefun.com

Therefore, the two tautomeric forms of CHT-1-CN were also considered as a result of this equilibrium reaction. The geometry optimizations of the four structures (two conformers and two tautomers) were performed at the B3LYP-D3/aug-cc-pVTZ level of theory using the ORCA program package 5.0[20,21]. The computed rotational constants, dipole moment components, and zero-point corrected relative energies along with the optimized structures are summarized in Table 1.
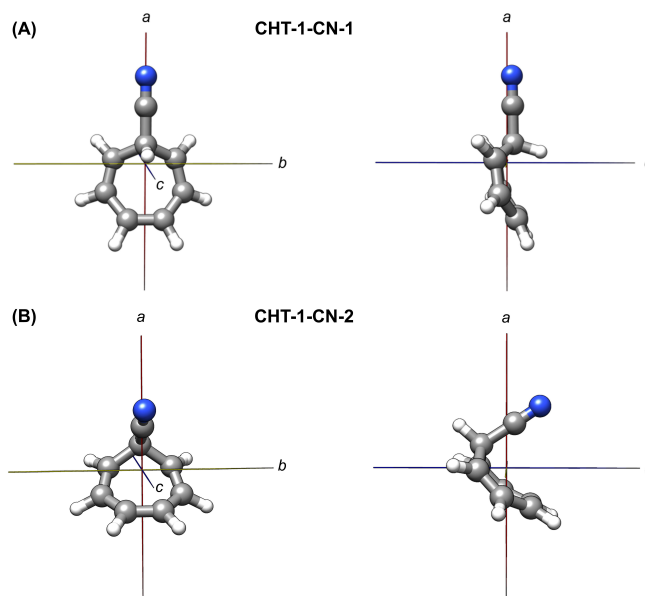

Fig. 1 Molecular structures and principal inertia axes of the lowest energy conformers (A) CHT-1-CN-1(top) and (B) CHT-1-CN-2 (bottom) in the ab plane (left) and in the ac plane (right).

Anharmonic frequency calculations were also performed for the lowest energy conformer to aid the analysis of the rotational spectra of the vibrationally excited states. The program package Gaussian 09[22] was used to perform structure optimization and anharmonic frequency calculations at the B3LYP-D3/aug-cc-pVTZ level of theory. In addition to the theoretical rotational constants corre-

sponding to vibrationally ground and vibrationally excited states, the anharmonic frequency calculations also provided theoretical quartic centrifugal distortion constants, which are of great relevance for the assignment in the high-frequency region (75-110 GHz).

4   Results and discussion

CHT-1-CN is a seven-membered ring molecule containing a cyano group attached to position 1 (sp^3-C) of the ring. The structures of the two lowest-energy conformers according to the geometry optimization calculations performed at the B3LYP-D3/aug-cc-pVTZ level of theory are shown in Figure 1. Due to the presence of an sp^3-hybridized carbon atom at position 1, the π electrons of the ring are not fully delocalized, giving the molecule a bent shape. Spectroscopically, CHT-1-CN is a near-oblate asymmetric top with Ray's asymmetry parameter $\kappa = \frac{2B-A-C}{A-C} = -0.79$ and -0.60 for conformer 1 and 2, respectively.

4.1   Vibronic ground state

Among the four different structures studied computationally (Table 1), only the two lowest energy structures were observed in our experimental conditions as the rest of the structures are substantially higher in energy with respect to the lowest energy one. Hereafter, the abbreviation CHT-1-CN-1 refers to the lowest energy conformer and CHT-1-CN-2 refers to the conformer next in energy. As expected, the rotational spectra recorded below 26
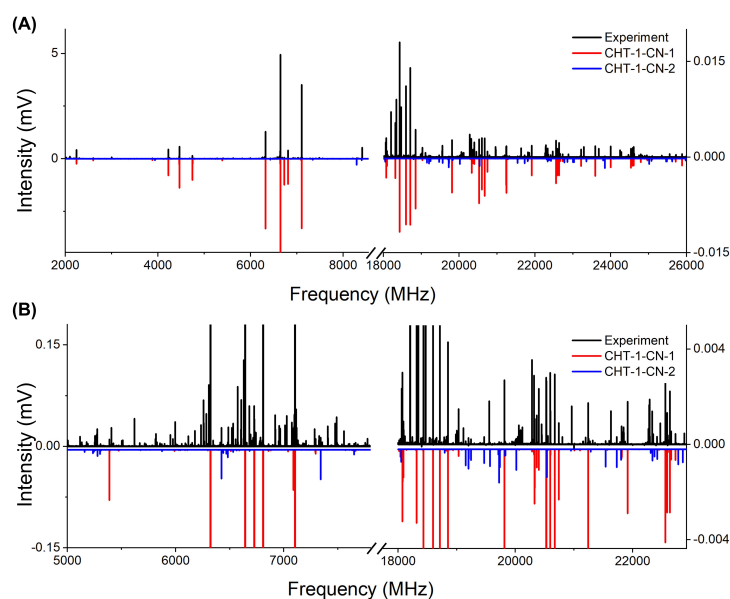

(A)

(B)

Fig. 2 Panel (A) shows the rotational spectra of the two lowest energy conformers in the frequency range of 2-8 and 18-26 GHz. The black trace represents the experimental spectra; the red and the blue traces correspond to the simulated spectra based on the fitted rotational constants of CHT-1-CN-1 and CHT-1-CN-2, respectively, at a rotational temperature of T_{rot}= 3 K. Panel (B) shows the zoom-in to emphasize the presence of the second conformer (in blue). The left and right intensity axes correspond to the experiments performed in the different frequency regions.

GHz (Figure 2) show resolvable hyperfine splitting (HFS) and the pattern of the HFS observed for the *a*-type transitions can

be found in Figure S1 in the supplementary information. The nuclear quadrupole coupling constants (NQCCs) obtained at the B3LYP-D3/aug-cc-pVTZ level of theory were used to simulate the HFS caused by the nuclear spin (I=1) of the ^{14}N nucleus. In the present work, ∼150 transitions with resolved HFS were assigned. The rotational spectrum in the W-band region displayed in Figure 3 does not show a resolvable HFS as the HFS collapses with the increasing rotational quantum number, J. For such transitions, the experimentally measured frequencies were assigned to the corresponding pure rotational transitions. In total, our data set contains 1272 and 123 assigned transitions for the vibronic ground states of CHT-1-CN-1 and CHT-1-CN-2, respectively. For
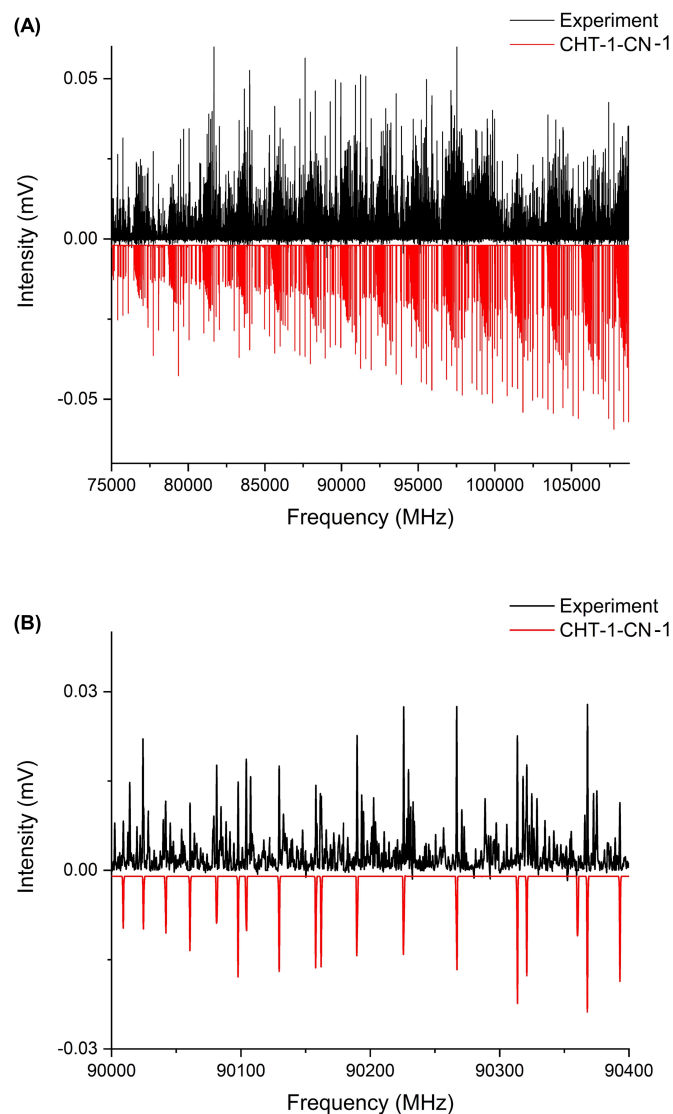

(A)

(B)

Fig. 3 Panel (A) shows the experimental (black trace) and simulated (red trace) rotational spectrum of CHT-1-CN-1 in the W-band region (75-110 GHz) recorded at about 323 K in a flow-cell setup. The simulated spectrum was obtained using the fitted rotational constants at a rotational temperature of T_{rot} ∼323 K. Panel (B) shows the zoom-in highlighting the well-resolved rotational transitions.

CHT-1-CN-1, the majority of the transitions were *a*-type transitions due to the high dipole-moment component along the *a*-

Table 2 Experimental and theoretical rotational parameters for the two lowest energy conformers, CHT-1-CN-1 and CHT-1-CN-2. The experimental rotational parameters were obtained as a result of the global fit in the frequency range 2-110 GHz and 2-26 GHz for CHT-1-CN-1 and CHT-1-CN-2, respectively. The rotational transitions were fit using Watson's A-reduction Hamiltonian in a I^r representation. The theoretical rotational parameters were calculated at the B3LYP-D3/aug-cc-pVTZ level of theory.

Rotational parameters	CHT-1-CN-1		CHT-1-CN-2	
	Experiment	Theory	Experiment	Theory
A^a/MHz	3538.12661(62)	3581.7	2232.1100(22)	2277.2
B/MHz	1251.39700(13)	1252.7	1702.8285(16)	1682.7
C/MHz	990.61360(11)	991.0	1573.6604(20)	1538.8
Δ_J^b/kHz	0.055512(30)	0.053	0.683(25)	0.657
Δ_{JK}/kHz	0.20096(13)	0.196	-1.176(81)	-1.457
Δ_K/kHz	0.830(20)	0.826	0.96(11)	1.224
δ_J/kHz	0.006708(17)	0.006	0.093(17)	-0.08
δ_K/kHz	0.27771(99)	0.267	$[0.145]^f$	0.145
χ_{aa}^c/MHz	-4.251(8)	-4.7	0.141(23)	0.09
χ_{bb-cc}/MHz	0.077 (17)	0.09	4.414(38)	4.85
σ^d/kHz	24.64		24.62	
No. of lines	1272		123	
J/K_a^e	54/38		5/7	

^{a} A, B, and C are the rotational constants

^{b} Δ_J, Δ_{JK}, Δ_K, δ_J, and δ_K are the quartic centrifugal distortion constants. The theoretical centrifugal distortion constants were estimated from the harmonic frequency calculation with a home-written python script.

^{c} χ_{aa}, χ_{bb}, and χ_{cc} represent the diagonal elements of the ^{14}N nuclear quadrupole coupling tensor.

^{d} Microwave root-mean-square deviation of the fit.

^{e} Maximum values of J and K_a assigned in the fit.

^{f} Parameters in square brackets were kept fixed to the corresponding theoretical value.

axis. In addition to this, some c-type transitions were also assigned but no b-type transitions could be observed due to a very low dipole-moment component along the b-axis. A global fit incorporating the rotational transitions from both low- and high-frequency regions was performed. For CHT-1-CN-2, both a-type and c-type transitions were assigned in 2-26 GHz due to the significant dipole moment components along the a- and c-axes, but no transitions for CHT-1-CN-2 could be assigned in the high-frequency region. This is due to a combination of factors, such as lower overall intensities observed in the flow cell experiment at 323 K and higher relative energy of CHT-1-CN-2 ($\sim$6 kJ/mol) and therefore lower abundance compared to the lowest energy conformer CHT-1-CN-1.

The experimental and theoretical rotational parameters for the vibronic ground state of both conformers are given in Table 2, and the list of assigned transitions of both conformers can be found in Tables S4.1-S4.3. For CHT-1-CN-1, the line list consists of rotational transitions from 2-110 GHz, while for CHT-1-CN-2, the line list comprises of rotational transitions from 2-26 GHz. As for the case of CHT-1-CN-1, analyzing high-frequency data sets allows for the accurate determination of the centrifugal distortion constants, which are crucial for the astronomical community, as this allows one to compute reliable rest frequencies in the higher frequency region more precisely than predictions based on the rigid rotor models alone. In this work, the transition frequencies of CHT-1-CN-1 were predicted up to 150 GHz based on the fitted rotational parameters, with the use of the SPCAT program[23]. For the vast majority of the predicted transitions, the uncertainties are well under 200 kHz. Besides the centrifugal distortion constants, the experimentally determined NQCCs, χ_{aa} and χ_{bb-cc}, are also important for interstellar searches, as the observation of the nuclear HFS can act as a further validation mechanism for interstellar detections. For example, the elucidation of the hyperfine splitting patterns of several interstellar molecules like cyanoallene[24] and benzonitrile[4] led to their conclusive identification in the ISM.

4.2 Structure determination

In addition to the lowest energy conformer CHT-1-CN-1, we also observed the rotational spectra of its singly substituted ^{13}C and ^{15}N isotopologues in natural abundances (1.1% and 0.4%, respectively) in the 2-26 GHz region. In the W-band region, no rotational transition arising from the heavy-atom isotopologues of CHT-1-CN-1 could be assigned in natural abundance. This is because, in the room-temperature measurement of CHT-1-CN, the vibrationally excited states are also populated, which increases the partition function of the molecule and thus decreases the intensities of the respective rotational transitions. For the second conformer CHT-1-CN-2 in the 2-26 GHz region, the overall intensity was not sufficient to observe its singly substituted ^{13}C and ^{15}N isotopologues in natural abundance.

The presence of a symmetry plane in CHT-1-CN-1 causes the effective natural abundance of the mirrored carbon atoms, labeled as ^{13}C(5), ^{13}C(6), and ^{13}C(7) (Figure 4, panels C and D), to be 2.2% instead of 1.1%. Since the change in the mass of the mirrored carbon atoms have the same effect on the mass distribution, the corresponding moments of inertia and hence the rotational constants are identical. All the assigned transitions arising from the singly substituted ^{13}C and ^{15}N isotopologues can be found
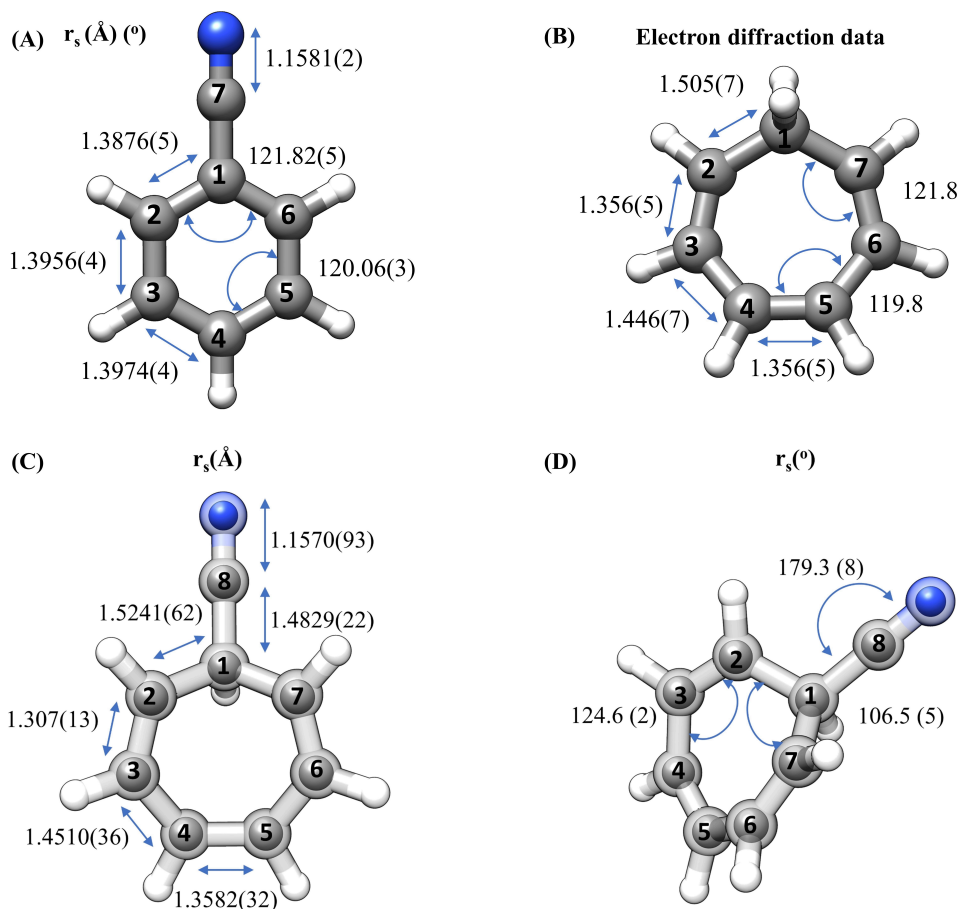
Fig. 4 Molecular structures of (A) benzonitrile[25], (B) cycloheptatriene[26], (C) and (D) CHT-1-CN-1 (experimental structure determined as a part of the current study). The inner bold spheres represent the r_s positions of the atoms, whereas the partially transparent backbone gives the theoretical r_e structure (B3LYP-D3/aug-cc-pVTZ level of theory). The bond lengths are given in panel (C) and the bond angles are given in panel (D). The bond distances and angles obtained by r_s are included where applicable. The numbering has been arranged in a way to facilitate a more effective comparison among the three molecules.

in Tables S5.1-S5.6 in the supplementary information along with the experimentally determined rotational parameters for all the observed isotopologues of CHT-1-CN-1 (Table S2). These experimentally obtained rotational constants were then utilized to determine the positions of each isotopically substituted atom with respect to the molecule's center of mass by employing Kraitchman's equations[27]. The comparison of the experimentally determined substitution structure (r_s) and the theoretical equilibrium structure (r_e) optimized at the B3LYP-D3/aug-cc-pVTZ level of theory is shown in Figure 4c and 4d. The bold spheres represent the experimentally determined atom positions (r_s) and the partially transparent backbone represents the equilibrium geometry (r_e) of the molecule.

It is informative to compare the structure of CHT-1-CN-1 to the ones of related molecules like benzonitrile[25] and cycloheptatriene (CHT)[10,26]. Figure 4 depicts the ring structures of these three molecules with their relevant bond lengths and bond angles shown in Table 3. For CHT, the values were taken from gas-phase electron diffraction data since rotational spectroscopy data on the structure determination of CHT is not available in the literature. The primary distinction in the structures of benzonitrile and CHT-

1-CN-1 is the degree of saturation of the bonds in the ring, and this impacts the resulting bond lengths. The structural differences between CHT and CHT-1-CN-1 arise from the substitution of a hydrogen atom with a CN group at the C(1) position. The differences in the degree of saturation between the above-mentioned systems also affect the aromaticity of the molecules. For example, benzonitrile is an aromatic molecule while CHT and CHT-1-CN-1 are non-aromatic, due to the presence of an sp^3- hybridized carbon atom at position 1. As a result, benzonitrile is a planar molecule, while CHT and CHT-1-CN-1 are bent in shape. The boat shape arrangement of CHT-1-CN-1 makes the angle at the sp^3-hybridized carbon atom C(1) the smallest (106.9°) and the bond length associated with C(1) be the longest $r_{C(1)-C(2)} = 1.5201(20)$ Å.

4.3 Vibrationally excited states

The flow-cell experiment performed with the W-band spectrometer (75-110 GHz) at $\sim$ 323 K allows for the observation of not only the vibronic ground state but also the low-lying vibrationally excited states. The population in these vibrationally excited states

Table 3 Comparison of bond lengths (in Å) and bond angles (in °) between the three structurally related molecules: CHT-1-CN-1 (this work), benzonitrile[25], and CHT[26].

Bond lengths (Å)				
CHT-1-CN-1[a]		CHT[b 26]	Benzonitrile[a 25]	
C(1)-C(2)	1.5241(62)	1.505(7)	C(1)-C(2)	1.3876(5)
C(2)-C(3)	1.308(13)	1.356(5)	C(2)-C(3)	1.3956(4)
C(3)-C(4)	1.4510(36)	1.446(7)	C(3)-C(4)	1.3974(4)
C(4)-C(5)	1.3582(32)	1.356(5)	C*-N	1.1581(2)
C(1)-C*	1.4829(22)			
C*-N	1.1570(93)			

Bond angles (°)				
CHT-1-CN-1[a]		CHT[b 26]	Benzonitrile[a 25]	
C(1)-C(2)-C(3)	120.4 (6)	121.8	C(1)-C(2)-C(3)	119.00(4)
C(2)-C(3)-C(4)	124.6(2)	127.2	C(2)-C(3)-C(4)	120.06(3)
C(3)-C(4)-C(5)	125.5(2)	119.8	C(3)-C(4)-C(5)	120.05(3)
C(2)-C(1)-C(7)	106.5(5)		C(2)-C(1)-C(6)	121.82(5)
C(1)-C*-N	179.3(8)		C(1)-C*-N	

[a] parameters determined via the r_s method
[b] parameters taken from an electron diffraction study of CHT in the gas phase
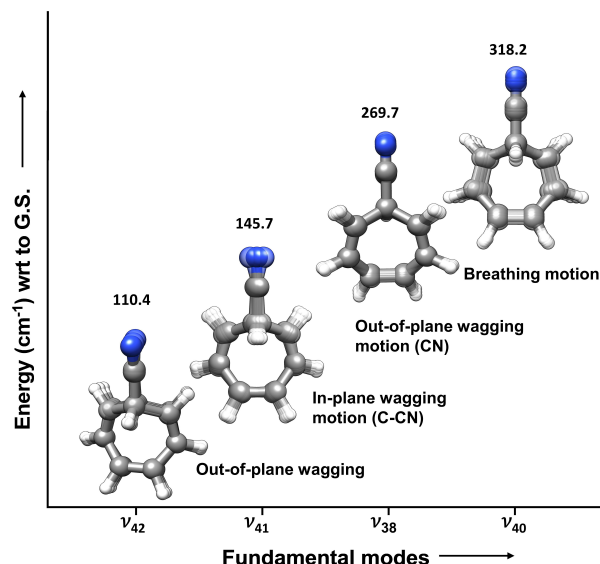* carbon atom of the cyano group

Fig. 5 A summary of the assigned fundamental vibrations of CHT-1-CN-1. The predominant motion for each mode is indicated by the overlapping transparent structures. The anharmonic energies are given with respect to the ground state and were calculated at the B3LYP-D3/aug-cc-pVTZ level of theory.

can be calculated using the Boltzmann distribution equation, which estimates the population distribution based on the temperature and the energy difference between the two states of interest. We present here the assignment of the six lowest energy vibrationally excited states of CHT-1-CN-1, namely v_{42}, v_{41}, $2v_{42}$, $v_{42} + v_{41}$, v_{40}, and v_{38}, within 500 cm^{-1} of energy difference relative to the ground state of CHT-1-CN-1. A brief description of the fundamental modes follows: v_{42} (110.4 cm^{-1}) is an out-of-plane bending motion, this can be seen as the movement of the C-CN bond and the ring C atoms in the *ac* plane; v_{41} (145.7 cm^{-1}) is an in-plane wagging motion along the C-CN bond in the *bc* plane; v_{40} (269.7 cm^{-1}) is an out-of-plane wagging motion of the CN group in the ac plane; v_{38} (318.2 cm^{-1}) is a breathing motion, shown by the periodic expansion and contraction of the ring structure. The spectral assignment of the vibrationally excited states was facilitated by anharmonic frequency calculations performed at the B3LYP-D3/aug-cc-pVTZ level of theory, the corresponding vibrational motions are depicted in Figure 5. The theoretical rotational constants obtained for each of the observed vibrationally excited states were shifted by the difference in the theoretical and experimental rotational constants obtained for the vibronic ground state at the same level of theory. The experimentally determined rotational constants and the number of assigned transitions for the four fundamental bands, as well as one overtone ($2v_{42}$) and one combination band ($v_{42} + v_{41}$), are listed in Table S3 in the supplementary information along with their derived rotational constants and anharmonic energies computed at the B3LYP-D3/aug-cc-pVTZ level of theory. The line lists of rotational transitions corresponding to the vibrationally excited states are given in Tables S6.1-S6.6 in the supplementary information.

4.4 Rotational and vibrational partition functions of CHT-1-CN-1

Interstellar searches for molecules of astronomical interest do not only require accurate rest frequencies but also information on the relative intensities of the rotational transitions. Partition functions can be used to predict the relative transition intensities at different rotational temperatures by direct summation over rotational energy levels. Further, the information on the partition functions is important for the calculation of the column densities[28]. The effect of temperature on the partition function is reflected in the observed transition intensities, as the increase in the temperature redistributes the population over the accessible vibrationally excited states resulting in overall lower signal intensities of the rotational transitions. A comparison of the simulated transition intensities at different temperatures for CHT-1-CN-1 is shown in Figure 6. The plot was made considering spin degeneracy equal to 0 ($2I + 1 = 1$, *i.e.*, the case where the hyperfine splitting is ignored).

Table 4 Rotational and vibrational partition functions calculated using the SPCAT program[29] for CHT-1-CN-1 across the standard range of temperatures as implemented in the JPL database[30].

CHT-1-CN-1			
T/K	$Q_{rot}[2I+1=1]^a$	Q_{vib}	$Q_{tot} = Q_{rot} \times Q_{vib}$
300	164124.64	4.623	758748.21
225	137771.51	3.41	469800.86
150	100473.94	2.167	217727.03
75	47757.85	1.221	58312.34
37.5	18374.49	1.018	18705.24
18.75	6541.21	1	6541.21
9.375	2314.62	1	2314.62
1.5	149.45	1	149.49

[a] $I = 0$ for ^{14}N, ignoring the HFS.

The experiment in the range of 75-110 GHz was performed at $\sim$323 K, therefore it is important to consider the vibrational partition function in addition to the rotational partition function. In Table 4, we list the rotational (Q_{rot}) and vibrational (Q_{vib}) partition functions of CHT-1-CN-1 calculated for the rotational quantum number J up to 60 without considering the HFS due to ^{14}N. The rotational partition functions were calculated using the SP-CAT program[31] across the standard temperatures as implemented in the Jet Propulsion Laboratory (JPL) database[30]. The vibrational contributions were calculated through direct summation of all of the vibrational modes up to 500 cm^{-1}. The total partition function (Q_{tot}) of the molecule in the electronic ground state is the product of Q_{rot} and Q_{vib}, as listed in Table 4.
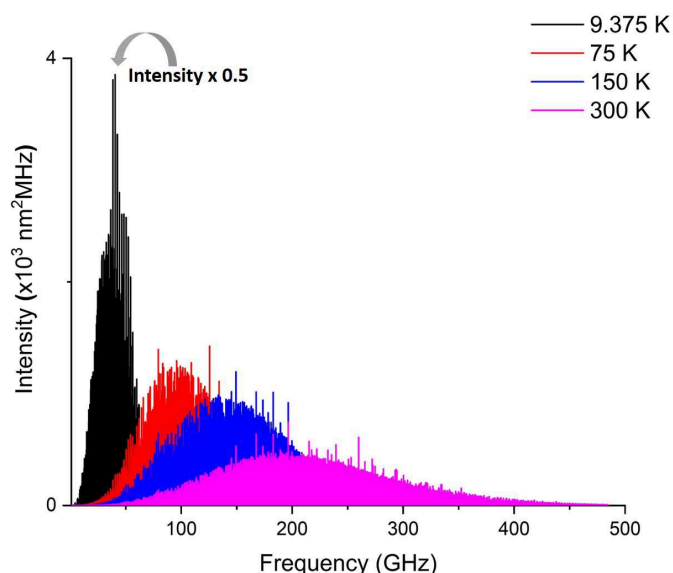

Fig. 6 Distribution of rotational transitions of CHT-1-CN-1 for four of the standard temperatures implemented in the JPL database[30]. The frequency simulation is made up to 500 GHz for the case of $2I+1 = 1$. Note that the intensity scale for the prediction at 9.375 K has been halved for clearer comparison with the predictions at higher temperatures.

5 Conclusions

This comprehensive investigation of the rotational spectra of 2,4,6-cycloheptatriene-1-carbonitrile led to the identification and assignment of the two lowest energy conformers, CHT-1-CN-1 and CHT-1-CN-2, in their vibronic ground states, including the assignment of the singly substituted ^{13}C and ^{15}N isotopologues in natural abundances. Additionally, six vibrationally excited states of CHT-1-CN-1 were also observed and characterized in the flow cell experiment at $\sim$323 K.

The analysis of the vibrationally excited states is an important task, as the detected vibrational states can serve as temperature probes in the region where they are observed, given that the ground state species has already been detected in that region. Moreover, it is useful for the simplification of complex astronomical datasets by eliminating lines from vibrationally excited states and isotopologues of already known molecules.

For the lowest energy conformer CHT-1-CN-1, the assignment

comprises of exact rotational frequencies in the 2-8, 18-26, and 75-110 GHz frequency ranges, leading to the determination of rotational parameters up to quartic distortion constants along with the nuclear quadrupole coupling constants. The accurate determination of centrifugal distortion constants allowed us to compute reliable rest frequencies in the high-frequency region (up to 150 GHz). For the vast majority of predicted transition frequencies, the uncertainties are well under 200 kHz, which makes this a reliable study for conducting astronomical searches. Rotational and vibrational partition functions were also calculated for the variety of temperatures as listed in the JPL database[30]. In addition to determining the gas-phase structure of CHT-1-CN-1 in the vibronic ground state, its structure can also be compared to other similar molecules like CHT and benzonitrile. The aromatic nature of benzonitrile explains the decrease in bond lengths in the ring structure as compared to those in CHT and CHT-1-CN-1, especially the ones including the C(1) carbon atom due to its sp^3 hybridization.

The astronomical detections of cyano-substituted five-membered and six-membered rings, cyanocyclopentadiene[6] and benzonitrile[4], respectively, make this cyano-substituted seven-membered ring (CHT-1-CN-1) a potential candidate to be detected in the ISM. Moreover, the electric dipole moment of CHT-1-CN-1 (4.3 D) makes it a favorable molecule to be searched for using radio astronomy. The astronomical search for CHT-1-CN-1 is suggested in TMC-1, where other cyclic molecules have been detected recently like benzonitrile[4], o-benzyne[32], cyclopentadiene and derivatives[33,34], and indene[33,35,36]. The comprehensive study of complex cyclic molecules like CHT-1-CN-1 opens up the possibility of investigating even more complex or cyclic molecules while testing the limits of radio astronomy.

Author Contributions

Gayatri Batra: Formal analysis, Validation, Investigation, Data curation, Writing - original draft, Writing - review & editing, Visualization. **Laura Pille**: Formal analysis, Validation, Investigation, Data curation, Writing - review & editing. **Benjamin E. Arenas**: Validation, Investigation, Data curation, Writing - review & editing, Project administration. **Melanie Schnell**: Resources, Writing - review & editing, Supervision, Funding acquisition, and Project administration.

Conflicts of interest

The authors declare that they have no known competing financial interests or personal relationships that could have appeared to influence the work reported in this paper.

Acknowledgements

Notes and references

1 B. E. Arenas, M. Fatima, C. Pérez, S. Fischer, A. L. Steber and M. Schnell, *The Astrophysical Journal*, 2021, **912**, 90.

2 M. C. McCarthy and B. A. McGuire, *The Journal of Physical Chemistry A*, 2021, **125**, 3231–3243.

3 M. C. McCarthy and B. A. McGuire, *The Journal of Physical Chemistry A*, 2021, **125**, 3231–3243.

4 B. A. McGuire, A. M. Burkhardt, S. Kalenskii, C. N. Shingledecker, A. J. Remijan, E. Herbst and M. C. McCarthy, *Science*, 2018, **359**, 202–205.

5 A. M. Burkhardt, R. A. Loomis, C. N. Shingledecker, K. L. K. Lee, A. J. Remijan, M. C. McCarthy and B. A. McGuire, *Nature Astronomy*, 2021, **5**, 181–187.

6 K. L. Kelvin Lee, P. B. Changala, R. A. Loomis, A. M. Burkhardt, C. Xue, M. A. Cordiner, S. B. Charnley, M. C. McCarthy and B. A. McGuire, *The Astrophysical Journal Letters*, 2021, **910**, L2.

7 K. L. Kevin Lee, B. A. McGuire and M. C. McCarthy, *Physical Chemistry Chemical Physics*, 2019, **21**, 2946–2956.

8 S. M. Fortman, I. R. Medvedev, C. F. Neese and F. C. De Lucia, *The Astrophysical Journal Letters*, 2010, **725**, L11.

9 V. Taquet, E. F. van Dishoeck, M. Swayne, D. Harsono, J. K. Jørgensen, L. Maud, N. F. W. Ligterink, H. S. P. Müller, C. Codella, K. Altwegg, A. Bieler, A. Coutens, M. N. Drozdovskaya, K. Furuya, M. V. Persson, M. L. R. van't Hoff, C. Walsh and S. F. Wampfler, *Astronomy & Astrophysics*, 2018, **618**, A11.

10 C. la Lau and H. de Ruyter, *Spectrochimica Acta*, 1963, **19**, 1559–1566.

11 S. S. Butcher, *The Journal of Chemical Physics*, 1965, **42**, 1833–1836.

12 W. Paulick, C. Jung, U. Kempka, J. Sühnel and K. Gustav, *Journal of Molecular Structure: THEOCHEM*, 1981, **85**, 235–240.

13 R. A. Creswell, *Journal of Molecular Spectroscopy*, 1974, **51**, 111–114.

14 D. Schmitz, V. A. Shubert, T. Betz and M. Schnell, *Journal of Molecular Spectroscopy*, 2012, **280**, 77–84.

15 C. Pérez, A. Krin, A. L. Steber, J. C. López, Z. Kisiel and M. Schnell, *The Journal of Physical Chemistry Letters*, 2016, **7**, 154–160.

16 M. Fatima, C. Pérez, B. E. Arenas, M. Schnell and A. L. Steber, *Physical Chemistry Chemical Physics*, 2020, **22**, 17042–17051.

17 B. E. Arenas, S. Gruet, A. L. Steber, B. M. Giuliano and M. Schnell, *Physical Chemistry Chemical Physics*, 2017, **19**, 1751–1756.

18 J. L. Neill, B. J. Harris, A. L. Steber, K. O. Douglass, D. F. Plusquellic and B. H. Pate, *Optics Express*, 2013, **21**, 19743.

19 L. M. Bateman, O. A. McNamara, N. R. Buckley, P. O'Leary, F. Harrington, N. Kelly, S. O'Keeffe, A. Stack, S. O'Neill, D. G. McCarthy and A. R. Maguire, *Org. Biomol. Chem.*, 2015, **13**, 11026–11038.

20 F. Neese, *WIREs Computational Molecular Science*, 2012, **2**, 73–78.

21 F. Neese, *WIREs Computational Molecular Science*, 2018, **8**, year.

22 M. J. Frisch, G. W. Trucks, H. B. Schlegel, G. E. Scuseria, M. A. Robb, J. R. Cheeseman, G. Scalmani, V. Barone, G. A. Petersson, H. Nakatsuji, X. Li, M. Caricato, A. V. Marenich, J. Bloino, B. G. Janesko, R. Gomperts, B. Mennucci, H. P. Hratchian, J. V. Ortiz, A. F. Izmaylov, J. L. Sonnenberg, D. Williams-Young, F. Ding, F. Lipparini, F. Egidi, J. Goings, B. Peng, A. Petrone, T. Henderson, D. Ranasinghe, V. G. Zakrzewski, J. Gao, N. Rega, G. Zheng, W. Liang, M. Hada, M. Ehara, K. Toyota, R. Fukuda, J. Hasegawa, M. Ishida, T. Nakajima, Y. Honda, O. Kitao, H. Nakai, T. Vreven, K. Throssell, J. A. Montgomery, Jr., J. E. Peralta, F. Ogliaro, M. J. Bearpark, J. J. Heyd, E. N. Brothers, K. N. Kudin, V. N. Staroverov, T. A. Keith, R. Kobayashi, J. Normand, K. Raghavachari, A. P. Rendell, J. C. Burant, S. S. Iyengar, J. Tomasi, M. Cossi, J. M. Millam, M. Klene, C. Adamo, R. Cammi, J. W. Ochterski, R. L. Martin, K. Morokuma, O. Farkas, J. B. Foresman and D. J. Fox, 2016.

23 Z. Kisiel, L. Pszczółkowski, I. R. Medvedev, M. Winnewisser, F. C. De Lucia and E. Herbst, *Journal of Molecular Spectroscopy*, 2005, **233**, 231–243.

24 F. J. Lovas, A. J. Remijan, J. Hollis, P. Jewell and L. E. Snyder, *The Astrophysical Journal*, 2006, **637**, L37.

25 J. Casado, L. Nygaard and G. Sørensen, *Journal of Molecular Structure*, 1971, **8**, 211–224.

26 M. Traetteberg, *Journal of the American Chemical Society*, 1964, **86**, 4265–4270.

27 J. Kraitchman, *American Journal of Physics*, 1953, **21**, 17–24.

28 J. G. Mangum and Y. L. Shirley, *Publications of the Astronomical Society of the Pacific*, 2015, **127**, 266–298.

29 Z. Kisiel, 2015.

30 H. Pickett, R. Poynter, E. Cohen, M. Delitsky, J. Pearson and H. Müller, *Journal of Quantitative Spectroscopy and Radiative Transfer*, 1998, **60**, 883–890.

31 H. M. Pickett, *Journal of Molecular Spectroscopy*, 1991, **148**, 371–377.

32 J. Cernicharo, M. Agúndez, R. Kaiser, C. Cabezas, B. Tercero, N. Marcelino, J. Pardo and P. De Vicente, *Astronomy & Astrophysics*, 2021, **652**, L9.

33 J. Cernicharo, M. Agúndez, C. Cabezas, B. Tercero, N. Marcelino, J. R. Pardo and P. De Vicente, *Astronomy & Astrophysics*, 2021, **649**, L15.

34 J. Cernicharo, R. Fuentetaja, M. Agúndez, R. I. Kaiser, C. Cabezas, N. Marcelino, B. Tercero, J. R. Pardo and P. de Vicente, *Astronomy & Astrophysics*, 2022, **663**, L9.

35 A. M. Burkhardt, K. L. K. Lee, P. B. Changala, C. N. Shingledecker, I. R. Cooke, R. A. Loomis, H. Wei, S. B. Charnley, E. Herbst, M. C. McCarthy *et al.*, *The Astrophysical Journal Letters*, 2021, **913**, L18.

36 M. L. Sita, P. B. Changala, C. Xue, A. M. Burkhardt, C. N. Shingledecker, K. L. K. Lee, R. A. Loomis, E. Momjian, M. A. Siebert, D. Gupta *et al.*, *The Astrophysical Journal Letters*, 2022, **938**, L12.